Available online at www.sciencedirect.com
ScienceDirect
Journal of Sound and Vibration 308 (2007) 674–682
JOURNAL OF SOUND AND VIBRATION
www.elsevier.com/locate/jsvi

A dynamic model for a rotating beam subjected to axially moving forces

Huajiang Ouyang[a,*], Minjie Wang[b]

[a]Department of Engineering, University of Liverpool, Liverpool L69 3GH, UK
[b]School of Mechanical Engineering, Dalian University of Technology, Dalian 116023, China

Accepted 28 March 2007
The peer review of this article was organised by the Guest Editor
Available online 11 June 2007

Abstract

This paper presents a dynamic model for the vibration of a rotating Timoshenko beam subjected to a three-directional load moving in the axial direction. The model takes into account the axial movement of the axial force component. The bending moment produced by this component acting on the surface of the beam is included in the model. The two other transverse force components are either of constant magnitude or a linear function of the local deflection. Lagrange's equations of motion for the modal coordinates are derived based on the assumed mode method. These equations are then solved by a fourth-order Runge–Kutta algorithm. Numerical examples are analysed. The effects of the axial force component and its induced bending moment, and the deflection-dependence of the moving forces on the dynamic behaviour of the system at various travelling speeds are investigated. It is found that the bending moment induced by the axial force component has a significant influence on the dynamic response of the rotating beam and hence must be considered in such problems as turning operations.

1. Introduction

Rotating beams are widely used in engineering. The dynamics of a rotating beam modelled as a Timoshenko beam, subjected to moving loads acting on the surface of the beam, is investigated. This dynamic model captures some basic features of a turning operation in machining, in which a cutting tool is moved in the axial direction against a work piece that is rotating quickly. In a real turning operation, the cutting force is a function of the deflection and its derivative(s), and is even dependent on the deflection history. The load in the current model is taken to be first of constant magnitude and then a linear function of the local deflection of the beam. A more sophisticated and realistic model of the moving load (the cutting force) will be studied in future.

The basic features of a dynamic model of turning should include a rotating member (usually a beam or a shell) excited by a force that moves in the axial direction. Lee et al. [1] and Katz et al. [2] are the first researchers to establish such a model. They studied the vibration of a rotating shaft as a beam based on Euler, Rayleigh and Timoshenko beam theories under a constant transverse load moving at constant velocity.

*Corresponding author. Department of Engineering, University of Liverpool, Liverpool L69 3GH, UK.
E-mail address: h.ouyang@liverpool.ac.uk (H. Ouyang).

0022-460X/$ - see front matter © 2007 Elsevier Ltd. All rights reserved.
doi:10.1016/j.jsv.2007.03.082

Dynamic response of a rotating shaft based on various beam theories and with various boundary conditions, subjected to various moving loads that travel at constant speed or non-constant speed, that are of constant magnitude or time-dependent or displacement-dependent or even random, were examined by a number of researchers [2–11].

Huang and Hsu [3] examined the resonance of a rotating cylindrical shell subjected to a moving transverse harmonic load. A rotating, simply supported Timoshenko beam excited by a distributed surface force travelling with acceleration was studied by Argento and Scott [4]. Han and Zu [5] developed a modal analysis approach for solving the problem of Katz et al. [2]. Zu and Han [6] investigated the vibration of a rotating Timoshenko beam with general boundary conditions and subjected to a moving transverse load, with the same approach of Han and Zu [5]. Lee [7] included the axial force (constant and non-moving) and found it had a significant effect on the magnitude of the dynamic response. A deflection-dependent force, used by Katz et al. [12], was introduced by Argento and Morano [8] for the moving load. Huang and Lee [9] dealt with a load moving repetitively forward and backward in the axial direction. Zibdeh and Juma [10] treated the moving load as a random force. Boundary conditions of nonlinear stiffness due to clearance in rolling bearings were considered by El-Saeidy [11]. He included bending moments in his moving load and introduced the finite element method to the study of rotating members subjected to moving loads. Chen and Ku [13] investigated the dynamic stability of a rotating shaft-disc system under an (non-moving) axial load. Sheu and Yang [14] studied the dynamic response of a spinning Rayleigh beam with mass eccentricity (but without moving load). Ouyang and Wang [15] included a moving bending moment in the dynamic model of a spinning Rayleigh beam.

In this paper, a dynamic model is presented for the vibration of a rotating shaft as a Timoshenko beam subjected to a load of three perpendicular components that acts on the surface of the shaft and moves in the axial direction at high speed. Because the shaft is modelled as a beam, the axial force component acting on the surface of the beam must be translated to the longitudinal axis of the beam and as a result a bending moment is generated. It will be seen later in the paper that this moment has a significant influence on both the magnitude and the frequencies of the vibration of the rotating beam, in particular at lower speeds. The effect of this moving axial force component is also included appropriately. The dynamic responses of this model are analysed with numerical examples.

2. Dynamic model

A circular beam rotating about its longitudinal axis, x, and subjected to a three-directional force moving along the x-axis is shown in Fig. 1. A rectangular coordinate system is fixed with the inertial frame.

The deflections of the rotating beam in the y and the z directions are denoted by v and w, and the angular rotations around y and z axes by ϕ and θ. Therefore, the shear strains on the cross section of the beam are

$$\varepsilon_{xy} = \frac{\partial v}{\partial x} - \theta, \quad \varepsilon_{xz} = \frac{\partial w}{\partial x} + \phi. \tag{1}$$

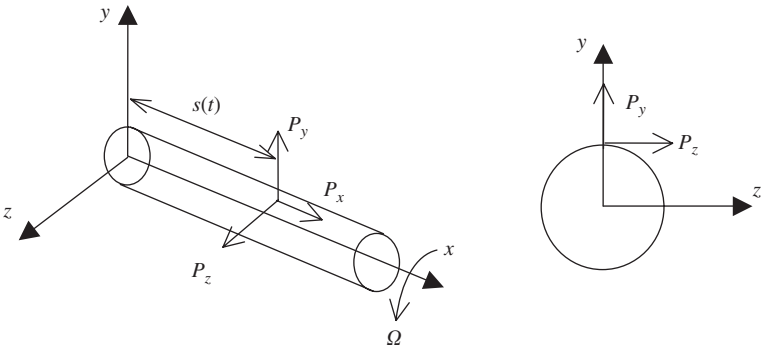

Fig. 1. A rotating shaft subjected to a moving load with three perpendicular forces.

The three-directional moving load acts on the surface of the beam and has to be translated to the neutral axis of the beam, as shown in Fig. 2.

When the axial force component P_x is translated to the longitudinal axis of the beam, a bending moment M_z is generated as [15]

$$M_z = -P_x r, \tag{2}$$

where r is the radius of the beam. As a normal practice in the studies of rotating beams subjected to moving loads [1–10], the axial and torsional vibrations of the beam are neglected in this paper and so will be absent in the subsequent equations.

Adapted from Ref. [13], the strain energy of a Timoshenko beam subjected to moving axial force P_x is

$$V = \frac{1}{2}\int_0^l EI\left[\left(\frac{\partial\phi}{\partial x}\right)^2 + \left(\frac{\partial\theta}{\partial x}\right)^2\right] dx + \frac{1}{2}\int_0^l kGA(\varepsilon_{xz}^2 + \varepsilon_{yz}^2)\, dx - \frac{1}{2}\int_s^l P_x\left[\left(\frac{\partial v}{\partial x}\right)^2 + \left(\frac{\partial w}{\partial x}\right)^2\right] dx, \tag{3}$$

where E is the Young's modulus and G the shear modulus, $I = \pi r^4/4$ the moment of area, $A = \pi r^2$ the cross-sectional area of the beam and k the shear coefficient.

The kinetic energy of the rotating Timoshenko beam is [13]

$$T = \frac{\rho}{2}\int_0^l \left\{A\left[\left(\frac{\partial v}{\partial t}\right)^2 + \left(\frac{\partial w}{\partial t}\right)^2\right] + I[\dot{\phi}^2 + \dot{\theta}^2 - 2\Omega(\phi\dot{\theta} - \theta\dot{\phi}) + 2\Omega^2]\right\} dx, \tag{4}$$

where Ω and ρ are the rotational speed and mass density of the beam.

The virtual work due to non-conservative forces:

$$\delta W = P_y\, \delta v(s,t) + P_z\, \delta w(s,t) + M_z\, \delta\theta(s,t). \tag{5}$$

The Lagrangian of the model is

$$L = T - V. \tag{6}$$

3. Mathematical formulation and computation

It is assumed that the deflections and rotations of the beam are:

$$\begin{aligned} v(x,t) &= \sum_{i=1}^{n} \varphi_i(x) a_i(t) = \boldsymbol{\varphi}^{\mathrm{T}}\mathbf{a}, \quad & w(x,t) &= \sum_{i=1}^{n} \varphi_i(x) b_i(t) = \boldsymbol{\varphi}^{\mathrm{T}}\mathbf{b}, \\ \phi(x,t) &= \sum_{i=1}^{n} \psi_i(x) c_i(t) = \boldsymbol{\psi}^{\mathrm{T}}\mathbf{c}, \quad & \theta(x,t) &= \sum_{i=1}^{n} \psi_i(x) d_i(t) = \boldsymbol{\psi}^{\mathrm{T}}\mathbf{d}, \end{aligned} \tag{7}$$

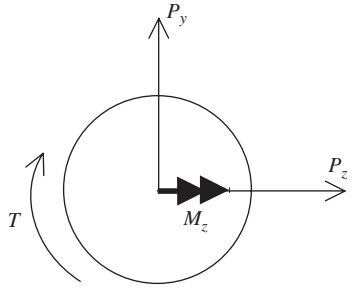

Fig. 2. Torque and bending moment generated from the three force components translated to shaft centre line.

where

$$\begin{aligned}
&\boldsymbol{\varphi}^{\mathrm{T}} = \{\varphi_1, \varphi_2, \ldots, \varphi_n\}, \quad &&\boldsymbol{\psi}^{\mathrm{T}} = \{\psi_1, \psi_2, \ldots, \psi_n\},\\
&\mathbf{a}^{\mathrm{T}} = \{a_1, a_2, \ldots, a_n\}, \quad &&\mathbf{b}^{\mathrm{T}} = \{b_1, b_2, \ldots, b_n\},\\
&\mathbf{c}^{\mathrm{T}} = \{c_1, c_2, \ldots, c_n\}, \quad &&\mathbf{d}^{\mathrm{T}} = \{d_1, d_2, \ldots, d_n\},
\end{aligned}$$

and $\varphi_i(x)$ and $\psi_i(x)$ are spatial functions that satisfies, respectively, the displacement boundary conditions and rotation boundary conditions of the beam, $a_i(t)$, $b_i(t)$, $c_i(t)$ and $d_i(t)$ are functions of time t to be determined.

Substitution of Eq. (7) into Eqs. (3–6) yields

$$\begin{aligned}
L = T - V = {} & \frac{\rho A}{2}(\dot{\mathbf{a}}^{\mathrm{T}}\mathbf{A}\dot{\mathbf{a}} + \dot{\mathbf{b}}^{\mathrm{T}}\mathbf{A}\dot{\mathbf{b}}) + \frac{\rho I}{2}(\dot{\mathbf{c}}^{\mathrm{T}}\mathbf{B}\dot{\mathbf{c}} + \dot{\mathbf{d}}^{\mathrm{T}}\mathbf{B}\dot{\mathbf{d}}) - \rho I\Omega(\dot{\mathbf{d}}^{\mathrm{T}}\mathbf{B}\mathbf{c} - \dot{\mathbf{c}}^{\mathrm{T}}\mathbf{B}\mathbf{d}) + \rho I\Omega^2 l\\
& - \frac{EI}{2}(\mathbf{c}^{\mathrm{T}}\mathbf{D}\mathbf{c} + \mathbf{d}^{\mathrm{T}}\mathbf{D}\mathbf{d}) - \frac{kGA}{2}(\mathbf{a}^{\mathrm{T}}\mathbf{C}\mathbf{a} - 2\mathbf{a}^{\mathrm{T}}\mathbf{E}\mathbf{d} + \mathbf{d}^{\mathrm{T}}\mathbf{B}\mathbf{d} + \mathbf{b}^{\mathrm{T}}\mathbf{C}\mathbf{b} + 2\mathbf{b}^{\mathrm{T}}\mathbf{E}\mathbf{c} + \mathbf{c}^{\mathrm{T}}\mathbf{B}\mathbf{c})\\
& + \frac{P_x}{2}[\mathbf{a}^{\mathrm{T}}\mathbf{C}_p(t)\mathbf{a} + \mathbf{b}^{\mathrm{T}}\mathbf{C}_p(t)\mathbf{b}]
\end{aligned} \tag{8}$$

and if the force components are functions of only t, then

$$\delta W = -\delta\mathbf{d}^{\mathrm{T}}\boldsymbol{\psi}(s)rP_x + \delta\mathbf{a}^{\mathrm{T}}\boldsymbol{\varphi}(s)P_y + \delta\mathbf{b}^{\mathrm{T}}\boldsymbol{\varphi}(s)P_z, \tag{9}$$

or if P_y and P_z are a linear function of local deflection [12] in the form of

$$P_y = \bar{P}_y - k_v v(s), \quad P_z = \bar{P}_z - k_w w(s), \tag{10}$$

then

$$\delta W = -\delta\mathbf{d}^{\mathrm{T}}\boldsymbol{\psi}(s)rP_x + \delta\mathbf{a}^{\mathrm{T}}\boldsymbol{\varphi}(s)[\bar{P}_y - k_v\boldsymbol{\varphi}^{\mathrm{T}}(s)\mathbf{a}] + \delta\mathbf{b}^{\mathrm{T}}\boldsymbol{\varphi}(s)[\bar{P}_z - k_w\boldsymbol{\varphi}^{\mathrm{T}}(s)\mathbf{b}], \tag{11}$$

where

$$\begin{aligned}
&\mathbf{A} = \int_0^l \boldsymbol{\varphi}(x)\boldsymbol{\varphi}^{\mathrm{T}}(x)\,\mathrm{d}x, \quad &&\mathbf{B} = \int_0^l \boldsymbol{\psi}(x)\boldsymbol{\psi}^{\mathrm{T}}(x)\,\mathrm{d}x, \quad &&\mathbf{C} = \int_0^l \boldsymbol{\varphi}'(x)\boldsymbol{\varphi}'^{\mathrm{T}}(x)\,\mathrm{d}x,\\
&\mathbf{C}_P(t) = \int_{s(t)}^l \boldsymbol{\varphi}'(x)\boldsymbol{\varphi}'^{\mathrm{T}}(x)\,\mathrm{d}x, \quad &&\mathbf{D} = \int_0^l \boldsymbol{\psi}'(x)\boldsymbol{\psi}'^{\mathrm{T}}(x)\,\mathrm{d}x, \quad &&\mathbf{E} = \int_0^l \boldsymbol{\varphi}'(x)\boldsymbol{\psi}^{\mathrm{T}}(x)\,\mathrm{d}x
\end{aligned} \tag{12}$$

and $\bar{P}_y$ and $\bar{P}_z$ are either of constant magnitude or functions of t, k_v and k_w are constant coefficients. In Eqs. (8) and (12), the dot and dash represent derivatives with respect to t and x, respectively.

Lagrange's equations of motion give

$$\begin{aligned}
&\rho A\mathbf{A}\ddot{\mathbf{a}} + [kGA\mathbf{C} - P_x\mathbf{C}_P(s)]\mathbf{a} - kGA\mathbf{E}\mathbf{d} = P_y\boldsymbol{\varphi}(s),\\
&\rho A\mathbf{A}\ddot{\mathbf{b}} + [kGA\mathbf{C} - P_x\mathbf{C}_P(s)]\mathbf{b} + kGA\mathbf{E}\mathbf{c} = P_z\boldsymbol{\varphi}(s),\\
&\rho I\mathbf{B}\ddot{\mathbf{c}} + 2\rho I\Omega\mathbf{B}\dot{\mathbf{d}} + (EI\mathbf{D} + kGA\mathbf{B})\mathbf{c} + kGA\mathbf{E}^{\mathrm{T}}\mathbf{b} = 0,\\
&\rho I\mathbf{B}\ddot{\mathbf{d}} - 2\rho I\Omega\mathbf{B}\dot{\mathbf{c}} + (EI\mathbf{D} + kGA\mathbf{B})\mathbf{d} - kGA\mathbf{E}^{\mathrm{T}}\mathbf{a} = -rP_x\boldsymbol{\psi}(s),
\end{aligned} \tag{13}$$

when the three force components are of constant magnitude or functions of only t, or

$$\begin{aligned}
&\rho A\mathbf{A}\ddot{\mathbf{a}} + [kGA\mathbf{C} - P_x\mathbf{C}_P(s) + k_v\boldsymbol{\varphi}(s)\boldsymbol{\varphi}^{\mathrm{T}}(s)]\mathbf{a} - kGA\mathbf{E}\mathbf{d} = \bar{P}_y\boldsymbol{\varphi}(s),\\
&\rho A\mathbf{A}\ddot{\mathbf{b}} + [kGA\mathbf{C} - P_x\mathbf{C}_P(s) + k_w\boldsymbol{\varphi}(s)\boldsymbol{\varphi}^{\mathrm{T}}(s)]\mathbf{b} + kGA\mathbf{E}\mathbf{c} = \bar{P}_z\boldsymbol{\varphi}(s),\\
&\rho I\mathbf{B}\ddot{\mathbf{c}} + 2\rho I\Omega\mathbf{B}\dot{\mathbf{d}} + (EI\mathbf{D} + kGA\mathbf{B})\mathbf{c} + kGA\mathbf{E}^{\mathrm{T}}\mathbf{b} = 0,\\
&\rho I\mathbf{B}\ddot{\mathbf{d}} - 2\rho I\Omega\mathbf{B}\dot{\mathbf{c}} + (EI\mathbf{D} + kGA\mathbf{B})\mathbf{d} - kGA\mathbf{E}^{\mathrm{T}}\mathbf{a} = -rP_x\boldsymbol{\psi}(s),
\end{aligned} \tag{14}$$

when the forces are defined by Eq. (10).

As can be seen from Eqs. (13) and (14), the moving axial force component has introduced a time-dependent stiffness term which in general reduces (when compressive) or increases (when tensile) the overall stiffness of the beam. The bending moment generated by this force component has added an extra term on the right-hand side of the fourth equation for the rotation of the beam's cross section about the z-axis, which is non-trivial.

The deflection-dependence of the forces adds extra terms in the stiffness matrix. Eqs. (13) and (14) will be solved using a fourth-order Runge–Kutta method.

4. Numerical results for constant forces

Numerical examples are presented for the dynamic responses of the shaft in terms of some parameters. The material and geometric properties of the simply supported circular shaft of Ref. [2] are taken so that results can be compared. $l = 1\,\text{m}$, $E = 2.07 \times 10^{11}\,\text{Pa}$, $G = 7.76 \times 10^{10}\,\text{Pa}$, $k = 0.9$, $\rho = 7700\,\text{kg m}^{-3}$. The fundamental frequency of the shaft when it is stationary is $\omega_1 = (\pi/l)^2\sqrt{EI/\rho A}$. The critical speed of the axial travel is $u_{\text{cr}} = (l/\pi)\omega_1 = (\pi/l)\sqrt{EI/\rho A}$. Non-dimensional parameters of $\alpha = u/u_{\text{cr}}$ (where u is the axial speed of the moving load), $\beta = \pi r/2l$ and $\bar{\Omega} = \Omega/\omega_1$ are often used in simulated examples [1,2]. $\bar{\Omega} = 2.5$. Ten beam modes ($n = 10$) are found to give good results and hence are used.

First of all, the case of $P_x = 0$, $P_y = -300\,\text{N}$, $P_z = 0$ is considered. The mid-span static deflection of the stationary shaft subjected to P_y at $x = l/2$ is $v_s = P_y l^3/48EI$. The numerical results of the dynamic responses in terms of the deflection ratios of v_p/v_s and w_p/v_s of two shafts of $r = 0.095\,\text{m}$ ($\beta = 0.15$) and $r = 0.019\,\text{m}$ ($\beta = 0.03$) are shown in Fig. 3, where v_p and w_p are instantaneous deflections of v and w at the location of the moving load.

These results look identical to those of the same problem reported in Ref. [7]. This indicates that the formulas in Eq. (13) and the derived Runge–Kutta algorithm are correct for this specific case.

Next, the dynamic responses of these shafts subjected to $P_x = 0$, $P_y = -300\,\text{N}$ and $P_z = -1100\,\text{N}$ travelling at different axial speeds are computed as a benchmark, shown in Fig. 4, for the subsequent comparisons with more complicated cases.

As P_z is several times higher than P_y, the dynamic response of w_p is also several times higher than v_p. The dynamic responses of w_p and v_p at different speeds u for shaft of $\beta = 0.15$ are similar in pattern, except for w_p and v_p at $\alpha = 0.11$. v_p at $\beta = 0.15$ and $\alpha = 0.11$ looks slightly out of place from other dynamic responses at $\alpha = 0.11$. Actually, its pattern is similar to those other dynamic responses in the sense that its first peak gets stretched upward slightly in comparison with other dynamic responses. Except for this one slightly peculiar case, the dynamic responses of the two shafts are also similar in pattern.

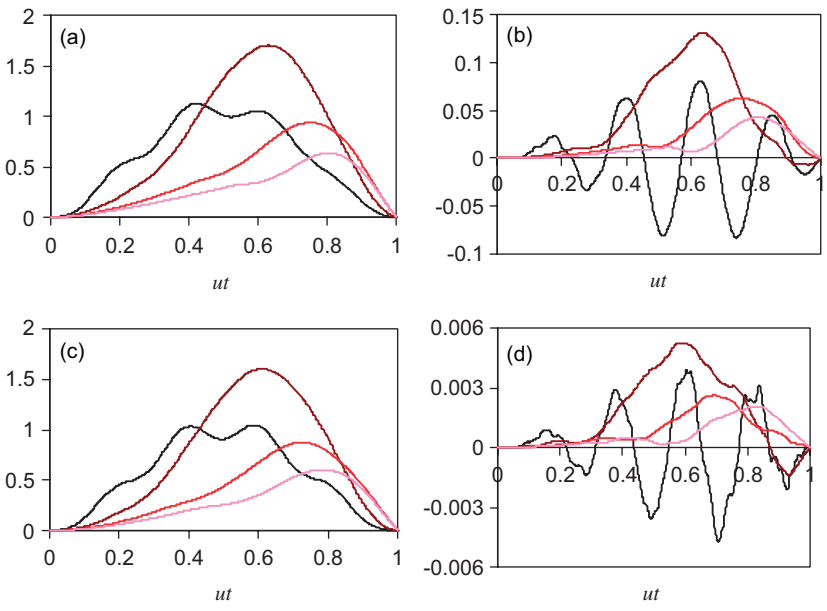

Fig. 3. Dynamic responses of the shaft subjected to $P_y = -300\,\text{N}$ moving at different speeds: (a) v_p/v_s at $\beta = 0.15$; (b) w_p/v_s at $\beta = 0.15$; (c) v_p/v_s at $\beta = 0.03$; and (d) w_p/v_s at $\beta = 0.03$. —— $\alpha = 0.11$, —— $\alpha = 0.5$, —— $\alpha = 1.1$, —— $\alpha = 1.5$.

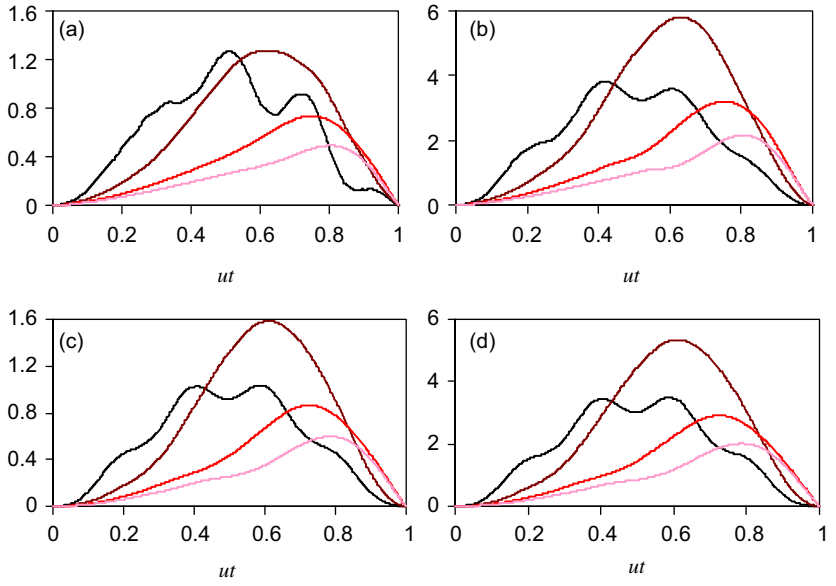

Fig. 4. Dynamic responses of the shafts subjected to two force components moving at different speeds (benchmark results): (a) v_p/v_s at $\beta = 0.15$; (b) w_p/v_s at $\beta = 0.15$; (c) v_p/v_s at $\beta = 0.03$; and (d) w_p/v_s at $\beta = 0.03$. The line codes are the same as in Fig. 3.

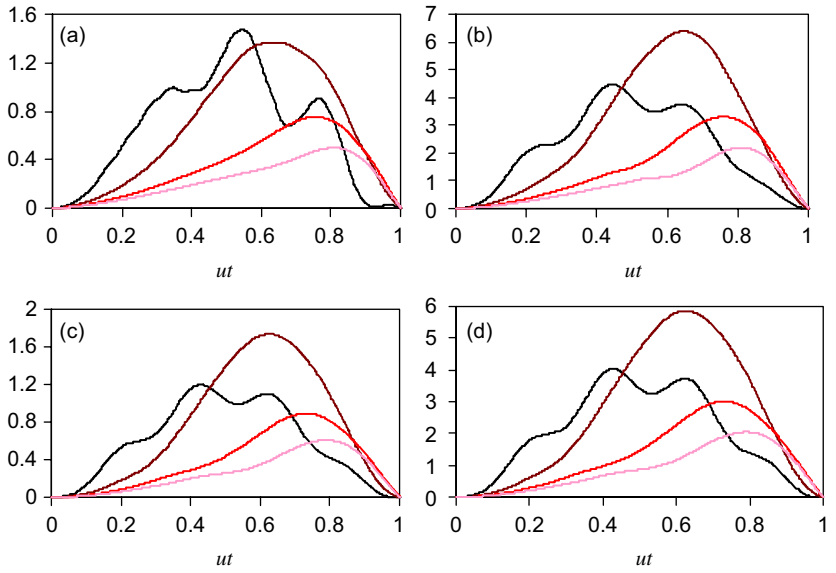

Fig. 5. Dynamic responses of the shafts subjected to three force components moving at different speeds ($P_x = 0.2P_{cr}$): (a) v_p/v_s at $\beta = 0.15$; (b) w_p/v_s at $\beta = 0.15$; (c) v_p/v_s at $\beta = 0.03$; and (d) w_p/v_s at $\beta = 0.03$. The line codes are the same as in Fig. 3.

The patterns of the dynamic responses of the shaft with the axial force and without are nearly the same (when M_z is ignored). A small increase in the height of the first peaks at $\alpha = 0.11$ is now obvious. The dynamic responses subjected to P_x increases for a compressive axial force ($P_x > 0$) and decreases for a tensile axial force ($P_x < 0$). Numerical results for $P_x = 0.2P_{cr}$ (where $P_{cr} = \pi^2 EI/l^2$ is the axial Euler buckling load of the shaft), $P_y = -300\,\mathrm{N}$ and $P_z = -1100\,\mathrm{N}$ are illustrated in Fig. 5.

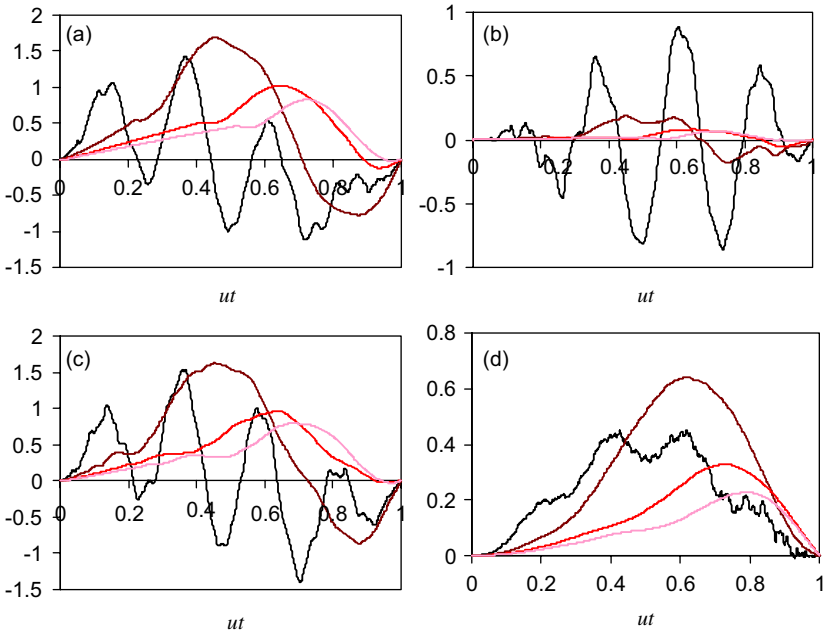

Fig. 6. Dynamic responses of the shafts subjected to three force components and the induced bending moment moving at different speeds ($P_x = 0.2P_{cr}$): (a) v_p/v_s at $\beta = 0.15$; (b) w_p/v_s at $\beta = 0.15$; (c) v_p/v_s at $\beta = 0.03$; and (d) w_p/v_s at $\beta = 0.03$. The line codes are the same as in Fig. 3.

Note that the P_x-induced moment M_z has not been considered in the above calculations. It has been ignored by other researchers. The results that exclude M_z are presented here so that they can be compared with the results of similar cases when M_z is included, in the following example.

Finally, M_z is now considered and all other data remains the same. Numerical results are presented in Fig. 6.

When the induced moment is considered, the dynamic responses experience rather drastic changes. The vibration magnitude increases by a large amount at low travelling speeds (v_p and w_p are now non-dimensionalised against a new mid-span static deflection of $v_s = P_y l^3/48EI + M_z l^2/16EI$, which is much larger than $P_y l^3/48EI$). Moreover, the dynamic responses are more eventful in the sense that there are more cycles of oscillations or smaller-amplitude faster vibrations at $\alpha = 0.11$ and they are no longer smooth. The dynamic responses now become negative when the forces travel to certain locations. At first glance, it may seem odd that Figs. 6a–c are similar in pattern but Fig. 6d is out of place. This should be clear from Fig. 7, where only P_x and M_z are present, so that the influence of the induced moment may be revealed. Notice that here $v_s = M_z l^2/16EI$.

As seen from Fig. 7, the dynamic responses of w_p produced by M_z for the shaft of $\beta = 0.03$ are relatively small. Therefore, the dynamic responses due to P_y and P_z play a big part in the results of Fig. 6d and hence Fig. 6d looks close to Fig. 5d in which M_z is neglected. In other words, the influence of M_z on w_p for the shaft of $\beta = 0.03$ is much less than in other cases with greater radii.

5. Numerical results for deflection-dependent forces

All the parameters used for the results of Fig. 5 are adopted here, except that the forces are now defined by Eq. (10). Following Katz et al. [12], a new parameter is introduced as $\gamma = k_v/\rho A l\omega_1^2$ and k_w is taken to be the same as k_v for the sake of simplicity. $\bar{P}_y = -300\,\mathrm{N}$ and $\bar{P}_z = -1100\,\mathrm{N}$. Numerical results obtained at three different values of γ are shown in Fig. 8.

Fig. 8 indicates that the greater γ is, the smaller deflection the shaft produces. This is expected according to Eq. (10).

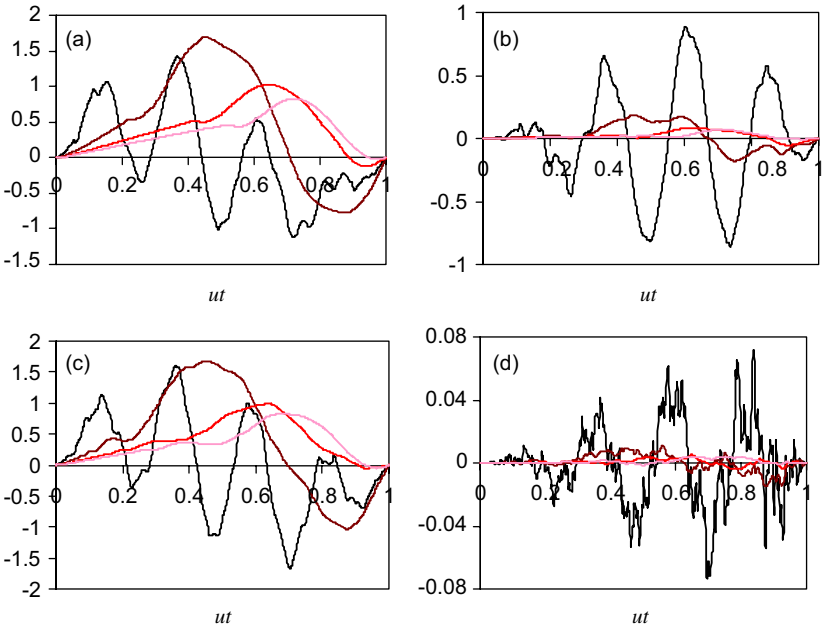

Fig. 7. The influence of M_z ($P_x = 0.2P_{cr}$, $P_y = 0$, $P_z = 0$): (a) v_p/v_s at $\beta = 0.15$; (b) w_p/v_s at $\beta = 0.15$; (c) v_p/v_s at $\beta = 0.03$; and (d) w_p/v_s at $\beta = 0.03$. The line codes are the same as in Fig. 3.

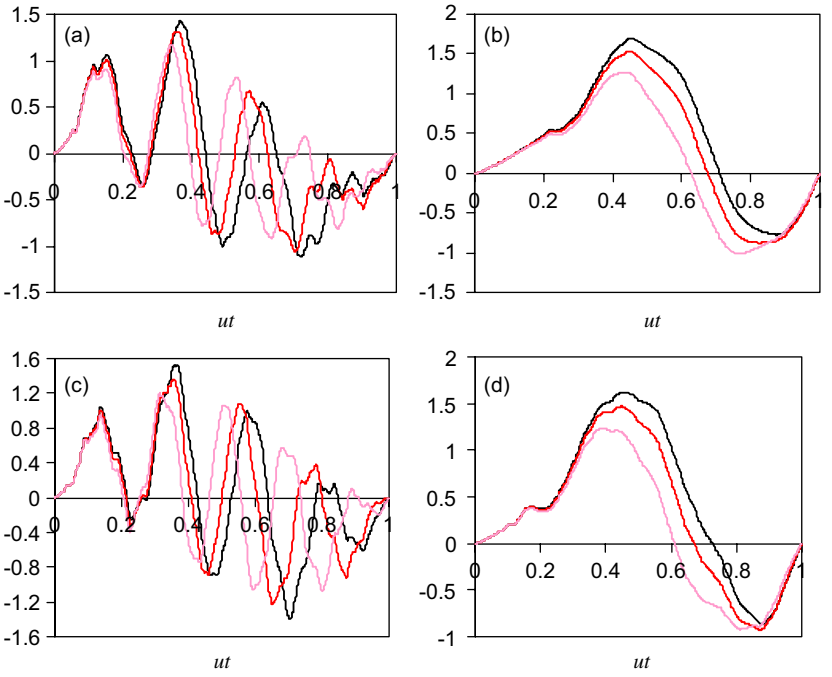

Fig. 8. The influence on γ on the dynamic responses: (a) $\alpha = 0.11$, $\beta = 0.15$; (b) $\alpha = 0.5$, $\beta = 0.15$; (c) $\alpha = 0.11$, $\beta = 0.03$; and (d) $\alpha = 0.5$, $\beta = 0.03$. —— $\gamma = 0$, —— $\gamma = 0.1$, —— $\gamma = 0.3$.

It is also clear from Fig. 8 that the magnitude of the dynamic responses varies with γ but their vibration patterns remain the same, which is consistent with the finding on a similar example [12] without the axial force-induced moment.

6. Conclusions

A dynamic model for a rotating Timoshenko beam subjected to a moving surface load of three force components (two transverse and one axial) is established. The bending moment induced by the axial force component acting on the surface of the shaft is included in the moving-load model. The two transverse force components of the moving load are modelled as of constant magnitude or a linear function of the local deflection of the beam. Numerical results show that with moving axial force, the deflection of the shaft increase when under compression and decreases when under tension, compared with the case of no axial force. When the axial-force-induced moving moment is included, the deflection of the beam increases by a great deal (under compression) and higher-frequency components also become much greater, in particular at relatively low speeds. The deflection-dependence of the forces changes the magnitude of the dynamic responses, but their vibration patterns are very similar.

Acknowledgements

Professor M. Wang is a visiting professor hosted by Dr H. Ouyang and the work is carried out in the first author's department.

References

[1] C.W. Lee, R. Katz, A.G. Ulsoy, R.A. Scott, Modal analysis of a distributed parameter rotating shaft, *Journal of Sound and Vibration* 122 (1987) 119–130.
[2] R. Katz, C.W. Lee, A.G. Ulsoy, R.A. Scott, The dynamic response of a rotating shaft subject to a moving load, *Journal of Sound and Vibration* 122 (1987) 134–148.
[3] S.C. Huang, B.S. Hsu, Resonant phenomena of a rotating cylindrical shell subjected to a harmonic moving load, *Journal of Sound and Vibration* 136 (1990) 215–228.
[4] A. Argento, R.A. Scott, Dynamic response of a rotating beam subjected to an accelerating distributed surface force, *Journal of Sound and Vibration* 157 (1992) 221–231.
[5] R.P.S. Han, J.W.Z. Zu, Modal analysis of rotating shafts: a body-fixed approach, *Journal of Sound and Vibration* 156 (1992) 1–16.
[6] J.W.Z. Zu, R.P.S. Han, Dynamic-response of a spinning Timoshenko beam with general boundary-conditions and subjected to a moving load, *ASME Journal of Applied Mechanics* 61 (1994) 152–160.
[7] H.P. Lee, Dynamic response of a rotating Timoshenko shaft subject to axial forces and moving loads, *Journal of Sound and Vibration* 181 (1995) 169–177.
[8] A. Argento, H.L. Morano, A spinning beam subjected to a moving deflection dependent load. 2: Parametric resonance, *Journal of Sound and Vibration* 182 (1995) 617–622.
[9] Y.M. Huang, C.Y. Lee, Dynamics of a rotating Rayleigh beam, *International Journal of Mechanical Sciences* 40 (1998) 779–792.
[10] H.S. Zibdeh, H.S. Juma, Dynamic response of a rotating beam subjected to a random moving load, *Journal of Sound and Vibration* 223 (1999) 741–758.
[11] F.M.A. El-Saeidy, Finite element dynamic analysis of a rotating shaft with or without nonlinear boundary conditions subjected to a moving load, *Nonlinear Dynamics* 21 (2000) 377–407.
[12] R. Katz, C.W. Lee, A.G. Ulsoy, R.A. Scott, Dynamic stability and response of a beam subjected to a deflection-dependent moving load, *ASME Journal of Vibration, Acoustics, Stress and Reliability in Design* 109 (1987) 361–365.
[13] L.-W. Chen, D.-M. Ku, Dynamic stability of a cantilever shaft-disk system, *ASME Journal of Vibration and Acoustics* 181 (1992) 326–329.
[14] G.J. Sheu, S.M. Yang, Dynamic analysis of a spinning Rayleigh beam, *International Journal of Mechanical Sciences* 47 (2005) 157–169.
[15] H. Ouyang, M. Wang, Dynamics of a rotating shaft subject to a three-directional moving load, *ASME Journal of Vibration and Acoustics* 129 (2007) 386–389.